NGC 4388 - SPECTRAL STUDIES OF THE FIRST SEYFERT 2 SEEN BY INTEGRAL

V. Beckmann[1,2], N. Gehrels[1], P. Favre[3,4], T. J.-L. Courvoisier[3,4], R. Walter[3,4], J. Malzac[5,6], and P.-O. Petrucci[7]

[1]NASA Goddard Space Flight Center, Code 661, Greenbelt, MD 20771, USA
[2]Joint Center for Astrophysics, Department of Physics, University of Maryland, Baltimore County, MD 21250

[3]INTEGRAL Science Data Centre, Chemin d'Écogia 16, 1290 Versoix, Switzerland
[4]Observatoire de Genève, 51 Ch. des Maillettes, 1290 Sauverny, Switzerland

[5]Centre d'Étude Spatiale des Rayonnements, 31028 Toulouse, France
[6]Institute of Astronomy, University of Cambridge, Madingley Road, Cambridge CB3 0HA, United Kingdom
[7]Laboratoire d'Astrophysique de Grenoble, BP 53X, 38041 Grenoble Cedex, France

ABSTRACT

We present first *INTEGRAL* and *XMM-Newton* observations of a Seyfert galaxy, the type 2 AGN NGC 4388. Several *INTEGRAL* observations performed in 2003 allow us to study the spectrum in the 20 – 300 keV range. In addition two *XMM-Newton* observations give detailed insight into the 0.2 – 10 keV emission. Comparison with previous observations by *BeppoSAX*, *SIGMA* and *CGRO*/OSSE show that the overall spectrum from soft X-rays up to the gamma-rays can be described by a highly absorbed ($N_H \simeq 2.7 \times 10^{23}\,\mathrm{cm}^{-2}$) and variable non-thermal component in addition to constant non-absorbed thermal emission ($T \simeq 0.8\,\mathrm{keV}$) of low abundance ($Z \sim 7\% Z_\odot$), plus a constant Fe K$\alpha$ and Kβ line. The hard X-ray component is well described by a simple power law with a mean photon index of $\Gamma = 1.7$. During the *INTEGRAL* observations the flux at 100 keV increased by a factor of 1.5. The analysis of *XMM-Newton* data implies that the emission below 3 keV is decoupled from the AGN and probably due to extended emission as seen in *Chandra* observations. The constant iron line emission is apparently also decoupled from the direct emission of the central engine and likely to be generated in the obscuring material, e.g. in the molecular torus.

Key words: galaxies: active; galaxies: individual (NGC 4388); gamma rays: observations; X-rays: galaxies.

1. INTRODUCTION

Seyfert 2 galaxies are among the optically faintest Active Galactic Nuclei (AGN) seen in the Universe. This is believed to be due to a geometrical effect. The emission of the super massive black hole at the AGN core is probably absorbed by a surrounding torus. The torus not only hides the broad line region, causing the characteristic Seyfert 2 optical spectra with narrow emission lines, but also absorbes most of the low X-ray emission. As the soft X-ray region is very sensitive to absorption in the line of sight, the study of the hard X-ray emission above $\sim 3\,\mathrm{keV}$ is a powerful tool to investigate the central engine of Seyfert 2 (Ghisellini, Haardt & Matt 1994). In addition to this the variation of the Fe Kα line seems to vary differently with respect to the continuum in several cases (Iwasawa et al. 2003; Fabian 1977; Malzac & Petrucci 2002), which might be caused by the interaction of the core emission with the absorbing and reflecting material.

At higher energies absorption becomes less important revealing the emission from the close environment of the central black hole. Comptonized hard X-ray radiation from a hot ($\sim 100\,\mathrm{keV}$) plasma presumably forms an accretion disk corona (Haardt et al. 1994), and Compton reflection of these hard X-rays on a cool accretion disk is observable (George & Fabian 1991; Magdziarz & Zdziarski 1995). In Seyfert 2 galaxies, reflection of the central radiation on the molecular torus often leads to an additional, possibly dominant, reflection component (Ghisellini, Haardt & Matt 1994).

NGC 4388 ($z = 0.00842$; Phillips & Malin 1982) is a good probe to test these scenarios, as it is one of the brightest Seyfert 2 galaxies at hard X-rays. This barred spiral of morphological class SB(s)b pec is located at $RA = 12^h25'46.7''$ and $DEC = 12°39'44''$ (J2000.0) with an apparent optical magnitude of $B = 11.9\,\mathrm{mag}$ and is a member of the Virgo galaxy cluster. The energy range up to $\sim 10\,\mathrm{keV}$ has been studied with X-ray missions like *ROSAT*

(Antonelli et al. 1997), *ASCA* (Iwasawa et al. 1997; Forster et al. 1999), *BeppoSAX* (Risaliti 2002), *RXTE* (Sazonov & Revnivtsev 2004), and lately with *Chandra* (Iwasawa et al. 2003). Spectral studies of NGC 4388 of the hardest X-ray energies up to several hundreds of keV have been performed by *SIGMA* (Paul et al. 1991), by the OSSE experiment (Johnson et al. 1993) on the *Compton Gamma Ray Observatory* (CGRO; Gehrels et al. 1993), and up to $\sim$ 150 keV by the Phoswich Detector System (PDS; Frontera et al. 1997) on-board *BeppoSAX* (Butler & Scarsi 1990; Boella et al. 1997). The two *BeppoSAX* observations in 1999 and 2000 showed a high energy spectrum with a power law of $\Gamma = 1.6$ and 1.5, respectively. Due to the energy range covered by the PDS it was only possible to give a lower limit for a possible high energy cut-off ($E_C > 109$ keV). The *INTEGRAL* mission (Winkler et al. 2003), launched in October 2002, offers the unique opportunity to study the entire spectrum from 3 keV up to several MeV simultaneously. NGC 4388 was the first Seyfert 2 galaxy detected by *INTEGRAL* in January 2003. In this paper we present data from several *INTEGRAL* observations and compare the results with previous *SIGMA*, OSSE, and *BeppoSAX* measurements. The data also allow us to study spectral variations between the 2003 observations. In addition *XMM-Newton* data are presented to study the connection with soft X-rays.

2. SIMULTANEOUS X-RAY AND GAMMA-RAY OBSERVATIONS

NGC 4388 was detected by *INTEGRAL* in the course of the 3C273 open time observation (Courvoisier et al. 2003a). Though NGC 4388 lies 10.4 degrees north of the quasar 3C273, valuable data for the Seyfert 2 galaxy were obtained due to the large field of view (FOV) of IBIS ($19° \times 19°$, partially coded FOV) and SPI ($35° \times 35°$, partially coded FOV), and because of the dithering observation strategy which is optimised for the spectrometer in order to allow a proper background determination. Observations were performed during seven *INTEGRAL* revolutions in January, June and July 2003 (Tab. 1). The total amount of exposure time is 512 ksec with 274 ksec and 238 ksec in the January and June/July campaign, respectively. Most of the observations were carried out in a dithering mode. 36 ksec of observation were carried out in staring mode, and are therefore only partly useful for SPI analysis, but they allow a more precise flux extraction from the ISGRI data. Due to the smaller FOV of the two X-ray monitors (JEM-X) and of the optical monitor (OMC) on-board *INTEGRAL*, NGC 4388 has not been observed by those instruments. We will discuss the *INTEGRAL* data mainly in terms of the two observation campaigns in January 2003 (JAN03) and June/July 2003 (JUN03).

obs. date start	rev.	SPI exp. time [sec]	point.	observation mode
05/01/03	28	80520	39	5×5
11/01/03	30	10558	2	staring
17/01/03	32	182643	43	5×5
16/06/03	82	20000	1	staring
06/07/03	89	152950	47	5×5
09/07/03	90	59989	17	5×5
18/07/03	93	5283	2	staring

Table 1. INTEGRAL observations

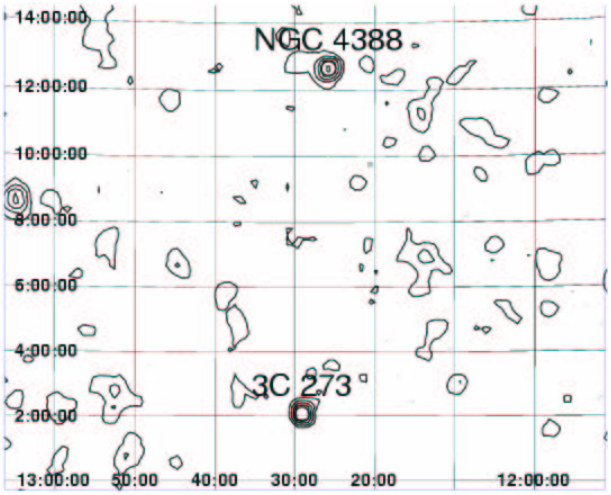

Figure 1. INTEGRAL/ISGRI significance contour map in the 20 – 40 keV energy band, based on the JUN03 data set. The coordinates are equatorial (J2000.0).

2.1. IBIS

The ISGRI spectrum has been extracted from ISGRI mosaics of the field created in 20 energy bands. The count rate and statistical error were extracted from the mosaic intensity and variance images for the ISGRI source position derived from the highest significant pixel of the mosaic in all energy bands. The mosaic image fully redistributes the pixel values of the sky images of individual science windows that were created using version 3.0 ot the Offline Science Analysis (OSA) software distributed by the ISDC (Courvoisier et al. 2003b). Pixel values are weighted according to vigneting and variance.

NGC 4388 was too faint to be seen by IBIS/PICsIT. Summing all available IBIS/ISGRI data together shows that NGC 4388 is detected up to 200 keV, though the data above 150 keV are consistent with zero flux on a 1σ level. A fit to a single power law gives a photon index of $\Gamma = 1.70^{+0.01}_{-0.01}$ and a flux of 7.8 ± 0.5 mCrab in the 20 - 40 keV energy band. Analysing the data according to the JAN03 and JUN03 campaign shows that the source was in a lower flux state in January 2003 with a similar spectral slope, while the June spectrum is steeper ($\Gamma = 2.06^{+0.23}_{-0.20}$) but has a higher flux. Note however that the spectral shape is still consistent with the

Table 2. Fit results for a single-power law model

Observation	Photon Index	F_X^a 20-40 keV	F_X^a 40-100 keV	F_X^a 100-200 keV	$\chi^2_\nu(dof)$
Jan.03 / ISGRI	$1.69\ ^{+0.57}_{-0.44}$	4.2 ± 0.9	7.2 ± 3.1	7.0 ± 5.9	0.63 (5)
Jan.03 / SPI	$1.56\ ^{+0.66}_{-0.53}$	9.7 ± 3.6	17.0 ± 7.8	19.9 ± 6.2	0.78 (2)
Jun.03 / ISGRI	$2.06\ ^{+0.23}_{-0.20}$	11.2 ± 1.4	14.1 ± 3.1	10.1 ± 8.8	1.00 (7)
Jun.03 / SPI	$1.36\ ^{+0.48}_{-0.47}$	4.9 ± 1.3	22.6 ± 8.7	30.9 ± 11.0	0.52 (5)
summed / ISGRI	$1.70\ ^{+0.01}_{-0.01}$	7.0 ± 0.4	11.7 ± 1.4	11.3 ± 3.3	1.69 (14)
summed / SPI	$1.68\ ^{+0.47}_{-0.35}$	7.7 ± 2.1	12.2 ± 4.8	12.6 ± 7.7	1.30 (4)

[a] un-absorbed flux in 10^{-11} erg cm^{-2} s^{-1}

$\Gamma = 1.7$ model on a 2σ level. For details see Table 2. Figure 1 shows the ISGRI significance contour map for the JUN03 observation, based on the 15 - 40 keV energy band.

2.2. SPI

In order to reduce the noise in the data reduction process of the SPI data, only those pointings were considered where NGC 4388 was less than 15 degrees off axis. This decreases the total amount of useable pointings to 122 with an exposure time of 178 ksec in JAN03 and 134 ksec in JUN03. OSA 3.0 has been applied, except for some updates. In the binning of the data SPIHIST 3.1.2 was used in order to avoid a known problem with the earlier version. In the case of the image reconstruction program SPIROS (Skinner & Connell 2003), we used the more recent version 6.0, applying the mean count modulation background model and the maximum likelihood method in order to find the best fitting model. Only single detector events were used for the analysis and the dead time correction has been applied for each detector individually, resulting in a mean dead time fraction per detector of 12.1%. We used an updated response function which takes into account the results from the in-flight calibration on the Crab. For details of the SPI analysis procedures see Diehl et al. (2003) and Beckmann (2002). The SPI spectrum of the combined data of JAN03 and JUN03 is well described by a single power law with photon index $\Gamma = 1.68^{+0.47}_{-0.35}$ and a flux of 9 ± 2.6 mCrab in the $20 - 40$ keV energy band, which is consistent with the ISGRI results. Analysing the JAN03 and JUN03 subset it turned out that the source strength is not sufficient for SPI to achieve a reasonable signal-to-noise for a spectrum. The results are shown in Table 2. The trend in the spectral evolution is opposite to the one detected in the ISGRI data, but the large error bars on the SPI results should be taken into account.

2.3. *RXTE*

The All Sky Monitor (ASM) on board the Rossi X-ray Timing Explorer (*RXTE*) scans about 80% of the sky every orbit. This offers an unique way to monitor the emission of bright X-ray sources like NGC 4388 in the $1.5 - 12$ keV energy range. We extracted fluxes from the RXTE/ASM data base. The fluxes have been averaged over the same time periods as the JAN03 and JUN03 *INTEGRAL* observations in order to have comparable results. The weighted mean of the JAN03 data was 3.5 ± 1.2 mCrab, while during the JUN03 campaign the flux was 2.2 ± 1.9 mCrab. Due to low statistics the analysis in the three different ASM bands did not give further information about the flux variability.

Table 3. XMM-Newton observations

obs. date start	MOS-1 exp. [sec]	MOS-2 exp. [sec]	PN exp. [sec]
07/07/02	9850	9937	4540
12/12/02	11667	11667	8291

3. *XMM-NEWTON* OBSERVATIONS

Two observations with *XMM-Newton* (Jansen et al. 2001) were performed in July and December 2002 as described in Table 3. Concerning the connection between the soft and hard X-ray emission, the most interesting data for our study come from the two MOS cameras (Turner et al. 2001) and from the PN detector (Strüder et al. 2001), as they cover the energy range $0.2 - 10$ keV. The data have been reduced using the *XMM-Newton* Science Analysis Software version 5.4.1 and the model fitting using XSPEC 11.3 was done simultaneously for the PN and MOS data. Both observations are well represented by a Raymond-Smith model (Raymond & Smith 1977) at energies below ~ 2.5 keV with low abundance (7% solar) and a temperature of about 0.8 keV, applying only Galactic absorption (2.7×10^{20} cm^{-2}). At harder X-rays, the spectrum is dominated by an absorbed power law. The column density of the neutral absorber is 2.7×10^{23} cm^{-2}. The power-law index is not well constrained by the *XMM-Newton* data because of the strong absorption, so the photon index of $\Gamma = 1.7$ measured at hard X-rays, has been applied. In addition, a Gaussian line at $6.39^{+0.01}_{-0.01}$ keV is apparent in both observations.

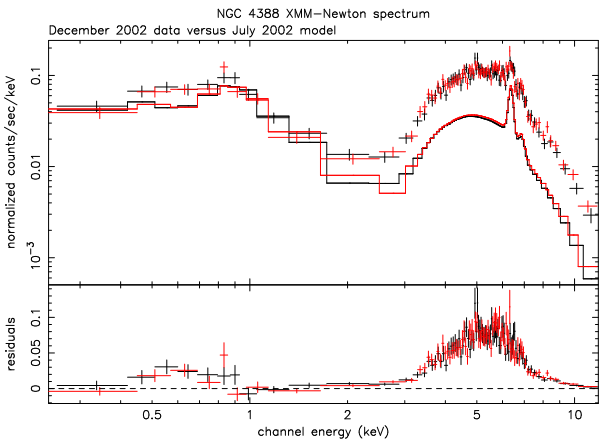

Figure 2. Comparison of XMM-Newton MOS data from December 2002 with respect to the model for the July 2002 EPIC/MOS data.

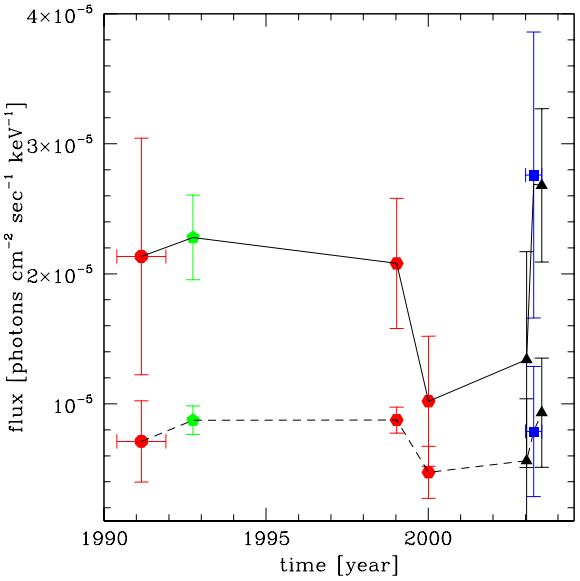

Figure 3. Lightcurve for NGC 4388 at 60 keV (upper solid line) and at 100 keV (lower dashed line). Data taken from SIGMA (circle), OSSE (pentagon), BeppoSAX/PDS (hexagon), SPI (square), and ISGRI (triangle).

Details of the fit are listed in Table 4. This is consistent with a recent measurement by *Chandra*, which showed an Fe line of centroid in 6.36 $^{+0.02}_{-0.02}$ keV (Iwasawa et al. 2003). The variation between the July and December data occurs mainly in the high energy part. This is clearly seen when comparing the December data with the model for the July data (Fig. 2). While there are little or no changes below $\sim 2.5\,\mathrm{keV}$, the spectrum varied significantly at higher energies. The iron fluorescence line at 6.39 keV was not affected by the variations. Another weak line is detectable at $6.89^{+0.13}_{-0.10}$ keV (probably Fe Kβ) with a flux about ten times lower than the Fe Kα line. In both *XMM* spectra there was no sign of a further line at 7.1 keV, as reported from *Chandra* data by Iwasawa et al. (2003).

Sazonov & Revnivtsev (2004) studied the *RXTE*/PCA slew data of AGN in the $3-20\,\mathrm{keV}$ energy band. This resulted for NGC 4388 in a luminosity of $L_{3-20\,\mathrm{keV}} = 4.5\times10^{42}\,\mathrm{erg\,s^{-1}}$, which is inside the range of the *XMM-Newton* observations in 2002 (extrapolated $L_{3-20\,\mathrm{keV}} = (2.8-7.0)\times10^{42}\,\mathrm{erg\,s^{-1}}$).

4. X-RAY TO GAMMA-RAY SPECTRUM

The *INTEGRAL* data alone do not allow us to reconstruct the complete X-ray spectrum of NGC 4388, mainly because the statistics of the ISGRI and SPI data do not constrain existing models.

Comparison with former observations by *SIGMA* (Lebrun et al. 1992), OSSE (Johnson et al. 1994), and *BeppoSAX*/PDS (Risaliti 2002) show a similar spectrum at hardest X-rays as observed with *INTEGRAL*. Measurements by BATSE gave a flux of $f_{20-100\,\mathrm{keV}} = (2.6\pm1.5)\times10^{-3}\,\mathrm{ph\,cm^{-2}\,s^{-1}}$, compared with an *INTEGRAL* value of $(2.7\pm0.3)\times10^{-3}\,\mathrm{ph\,cm^{-2}\,s^{-1}}$. This indicates that the soft gamma-ray spectrum does not vary dramatically as shown in the lightcurves for the 60 keV and 100 keV flux in Fig. 3. The flux measurements are consistent on a 2σ level and the spectral shape is conserved during the 13 years of various observations.

In order to extend the spectrum into the energy range below 20 keV we added the two *XMM-Newton* EPIC data sets, described in the previous section.

The data were fit simultaneously in XSPEC 11.3 applying the same model as for the *XMM* data alone: a Raymond-Smith model for a hot plasma with Galactic absorption, an absorbed power law, plus a Gaussian emission line. Figure 4 shows the combined photon spectrum of NGC 4388. The fit, which allowed for flux variations between the various non-simultaneous observations (see Sect. 5), gave a $\chi^2_\nu = 1.41$ for 1431 degrees of freedom. The normalisation factors are in the range 2.5 to 4.2 relative to the *XMM-Newton* July 2002 data. The power law, dominating the emission above $\sim 2.5\,\mathrm{keV}$, has a photon index of $\Gamma = 1.65^{+0.04}_{-0.04}$ and an absorption of $N_H = 2.73^{+0.07}_{-0.07}\times10^{23}\,\mathrm{cm^{-2}}$. Figure 5 shows the combined spectrum in $E^2 f_E$ versus E.

Using a more complicate model with a cut-off power law plus reflection from cold material (the so-called PEXRAV model; Magdziarz & Zdziarski 1995) instead of the simple power law, does not improve the fit significantly. Applying a single-power law plus an unresolved set of lines, represented by a broad Gaussian line around 1 keV, instead of the Raymond-Smith component does not give acceptable fit results ($\chi^2_\nu \gg 2.0$).

Using only the high energy ($> 20\,\mathrm{keV}$) data gives a

Table 4. Fit results for the XMM-Newton EPIC data

Observation	$T[kT]$	abundance	N_H $[10^{23}\,\mathrm{cm}^{-2}]$	$f_{\mathrm{Fe\,K}\alpha}$ $[10^{-5}\,\mathrm{ph\,cm}^{-2}\,\mathrm{s}^{-1}]$	EW [eV]	σ [eV]	$\chi^2_\nu(dof)$
July 2002	$0.81^{+0.04}_{-0.05}$	$0.08^{+0.03}_{-0.02}$	$2.45^{+0.20}_{-0.21}$	6.7 ± 1.2	566	67 ± 16	1.06 (526)
Dec. 2002	$0.80^{+0.03}_{-0.03}$	$0.06^{+0.01}_{-0.01}$	$2.79^{+0.07}_{-0.07}$	7.8 ± 1.4	220	69 ± 12	1.25 (861)

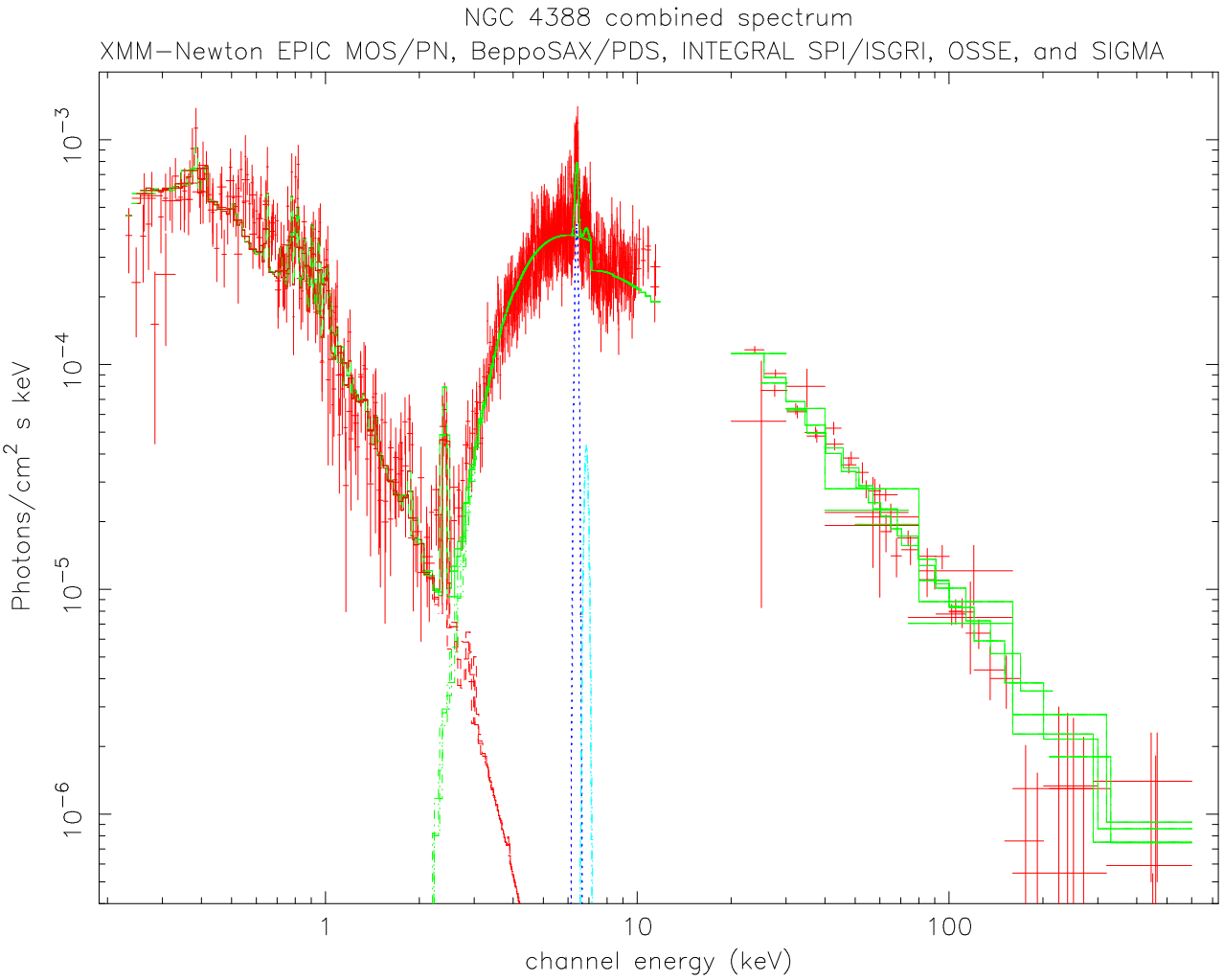

Figure 4. NGC 4388 combined photon spectrum, including XMM-Newton EPIC MOS/PN, BeppoSAX PDS, CGRO OSSE, SIGMA, and INTEGRAL ISGRI/SPI. The high energies are dominated by the highly absorbed component (sufficiently modeled by a single power law) plus the Kα and Kβ iron fluorescence lines, while the lower energies show emission characteristic for a hot plasma with low abundance. XMM data from July 2002 are not shown in this plot for better visibility.

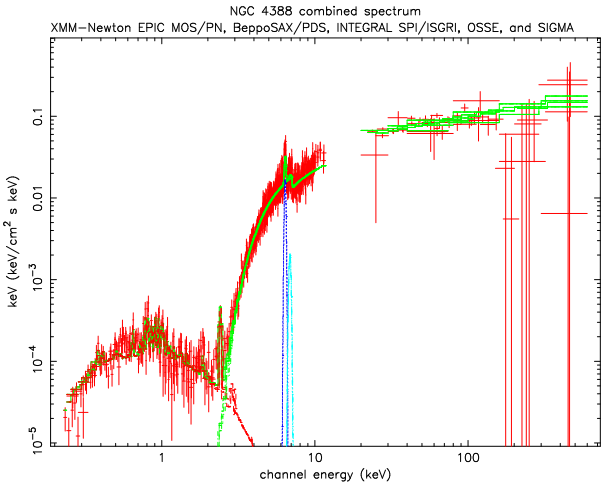

Figure 5. NGC 4388 combined spectrum in $E^2 f_E$ vs. E. The data cannot confirm or disprove the existence of a high energy cut-off.

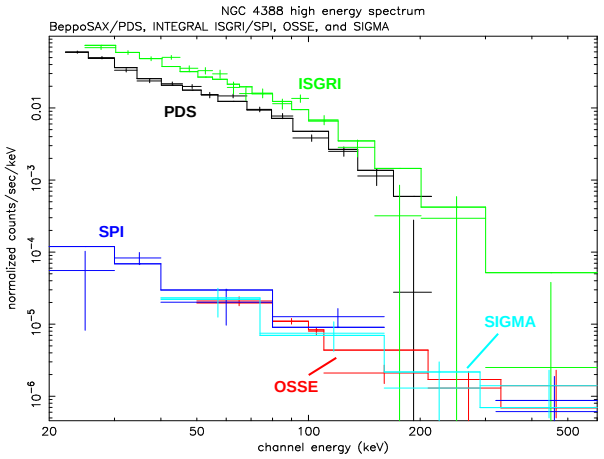

Figure 6. NGC 4388 combined high energy spectrum, including BeppoSAX PDS, CGRO OSSE, SIGMA, and INTEGRAL ISGRI/SPI. The spectrum is shown in instrument dependent counts s^{-1} keV^{-1}.

single power law with $\Gamma = 1.72^{+0.05}_{-0.05}$ with $\chi^2_\nu = 1.5$ (Fig. 6). Also in this energy region alone the more complex PEXRAV model does not give a significantly better fit. Statistics do not allow us to distinguish between a single power law and a PEXRAV model. The differences are smaller than the 1σ error bars of the spectra as seen in Fig. 6 and Fig. 5.

5. DISCUSSION

The combination of the *INTEGRAL* data with previous observations by *XMM-Newton*, *BeppoSAX*, *CGRO*, and *SIGMA* shows that the spectrum from 0.2 keV up to several hundred keV is well represented by a thermal Raymond-Smith model with only Galactic absorption applied, plus a highly absorbed ($N_H \simeq 2.7 \times 10^{23}\,cm^{-2}$) power law like emission ($\Gamma = 1.7$), and a Gaussian line to model the iron fluorescence line at 6.39 keV. The results are consistent with previous studies of NGC 4388 using subsets of these data (Risaliti 2002; Lebrun et al. 1992). Also observations with *Chandra* (Iwasawa et al. 2003) and *ASCA* (Iwasawa et al. 1997; Forster et al. 1999) show a similar spectral behavior.

The fact that the data of the different missions give an acceptable fit using the same normalisation is based on the fact that the error bars in the high energy domain are still rather large. But the good correspondence between the ISGRI and SPI data leads to the assumption that the *INTEGRAL* calibration is reasonable and that normalisation problems as reported e.g. in Courvoisier et al. (2003) are solved, although the large error bars on the high energy flux measurements (Fig. 3) still leave open the possibility of some errors in the calibration.

The spectral data of NGC 4388 do not drop drastically above 200 keV, but are not of high enough significance to distinguish whether there is a cut-off, as expected from Comptonisation models (Petrucci et al. 2001). The *XMM-Newton* data show variability only in the energy region above ~ 2.5 keV. This variability cannot be explained by a change in the absorption column density. But using the same model parameters of the July observation (Tab. 4) for the December 2002 data and allowing the normalization of the single power-law to vary, shows that a flux increase by a factor of 3.4 is sufficient to model the December data ($\chi^2_\nu = 1.1$; Fig. 2). The spectral shape of the power law, which describes the hard X-rays, the Fe Kα line strength, and the soft X-ray component does not seem to vary strongly.

The observed spectrum can be compared to the one derived by Ghisellini, Haardt, & Matt (1994) based on Monte-Carlo simulations for a Seyfert galaxy with inclination $i = 60° - 63°$, column density of $10^{24}\,cm^{-2}$ and a torus with half-opening angle of $\Theta = 30°$. Based on these assumptions, an equivalent width of the iron fluorescence line of the order of $EW \sim 100$ eV would be expected, which would also mean a parallel evolution of the line flux with respect to the continuum. But the Fe Kα does not show variability, while the underlying continuum varies by a factor of ~ 4 in the line region (see Fig. 7). The line flux of $(6.7 \pm 1.2) \times 10^{-5}$ ph cm^{-2} s^{-1} and $(7.8 \pm 1.4) \times 10^{-5}$ ph cm^{-2} s^{-1} for the July and December measurement is also consistent with the one measured by *Chandra* ($(9.3 \pm 1.9) \times 10^{-5}$ ph cm^{-2} s^{-1}; Iwasawa et al. 2003). The equivalent width therefore varied strongly ($EW = 190 - 720$ eV). The exception from this rule is the 1993 ASCA observation, which revealed a high continuum flux with simultaneous high line flux. But the rather stable line flux over several years with simultaneous strong variations of the underlying continuum implies that the line emitting region is separated from the continuum source of the object by several light years. A similar behavior has been observed in *RXTE* spectra of Seyfert 1 galaxies, where the Fe Kα line also varies less strongly than the broadband continuum (Markowitz, Edelson, &

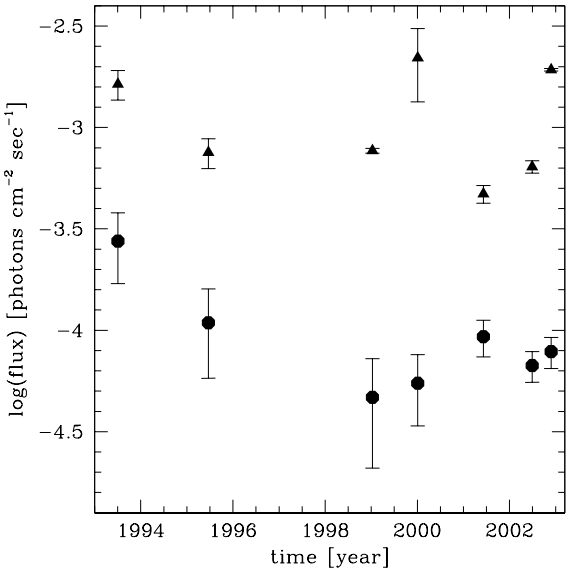

Figure 7. Flux in the 2-10 keV band (triangles) and of the 6.4 keV Fe Kα line (circles) measured by ASCA (1993 and 1995), BeppoSAX (1999 and 2000), Chandra (2001), and XMM-Newton (2002). The underlying continuum is highly variable, while the line flux shows no significant variation, except for the ASCA measurement in 1993.

Vaughan 2003).

Another difference of the spectrum observed here to the simulated one by Ghisellini, Haardt, & Matt (1994) is the fact that the spectrum of NGC 4388 does not seem to have a cut-off in the hard X-rays. This could be caused by a higher temperature of the corona ($\gg 100$ keV) in the case of NGC 4388. A reflection component is not detectable in the X-rays, which might be a hint for a non isotropic radiation or, generally speaking, a more complex geometry (see e.g. George & Fabian 1991). Apparently there is no scattering of the hard X-rays away from the line of sight. This indicates that in the case of NGC 4388 we indeed observe the unscattered emission of the central engine at hard X-rays. Also no decline due to Klein-Nishina processes appears above 50 keV.

The constant soft X-ray emission is most likely not linked to the AGN. This is also supported by the fact, that this emission is extended, as has been reported from *ROSAT*/HRI measurements (Matt et al. 1994) and lately from *Chandra* (Iwasawa et al. 2003). The low abundance in the extended emission has been seen already in the *ASCA* observations, though with much larger uncertainties ($Z = 0.05^{+0.35}_{-0.03} Z_{\odot}$; Iwasawa et al. 1997). Iwasawa et al. (2003) argue that the extended emission at low engergies is more likely to originate from photoionized plasma. Even though it is not possible, based on the *XMM-Newton* data presented here alone, to give a preference to a thermal or photoionized plasma, the latter one has the advantage of avoiding the low abundance in the vicinity (within several kpc) of the AGN core. The *Chandra* data also allowed a space resolved study at soft X-rays, which was not possible with *XMM*. We therefore refer to the more simple model, applied to the data presented here, which gives sufficient good fit results.

The *INTEGRAL*/ISGRI measurements indicate that a lower flux in the soft gamma-ray region is accompanied by a harder spectrum, but the errors on the spectral slope measurement are too large to be statistically significant. Off-axis effects are unlikely to play a role in the flux difference, as both observations, JAN03 and JUN03, were carried out in the same observation mode around the same center point. Since the SPI data at the same time show the contrary spectral evolution, it is likely that the spectral slope did not change and that there is only a change in flux ($20 - 200$ keV) by a factor of ~ 2.

This variation is not seen in the *RXTE*/ASM data, which cover the softer energy range (1.5 – 12 keV). Note also the large error values, which are consistent with no flux variation for the *INTEGRAL* and *RXTE* data.

6. CONCLUSION

The complex X-ray spectrum of NGC 4388 is composed out of three major components:

- **Hot plasma component**: Emission below $\sim$ 2.5 keV is dominated by emission of a hot (10^7 °K), optically thin plasma with low abundance (about 7 % solar). This component does not seem to be variable. In *ROSAT*/HRI and *Chandra* observations this emission appeared to be an extended X-ray nebula out to several kpc from the AGN. *Chandra* observations imply that this component might be due to photoionized gas.
- **Non-thermal emission**: Emission above $\sim$ 2.5 keV follows a highly absorbed ($N_H \sim 2.7 \times 10^{23}$ cm^{-2}) power law with photon index $\Gamma = 1.7$. While the flux of this component varied by a factor $\simeq 4$ over the past ten years, the spectral shape has been constant within the error bars.
- **Iron line emission**: The Fe Kα fluorescence line at 6.39 keV and the Kβ at 6.9 keV, both consistent with the redshift of the AGN. The former had a constant flux of $\sim 7.5 \times 10^{-5}$ ph cm^{-2} s^{-1} from 1995 to 2002. No line broadening is seen. The iron line emission is decoupled from the broadband continuum, similar to the behavior observed in Seyfert 1 galaxies (Markowitz, Edelson, & Vaughan 2003).

The *INTEGRAL* data do not allow to constrain the model on the high energy emission, i.e. there is no sign of a Compton reflection component or a cutoff at higher energies.

Following the observations reported here, NGC 4388 was studied in a dedicated *INTEGRAL* observation, which was performed in staring mode in revolution 94 in July 2003. Though staring mode observations usually do not produce useful SPI spectra for sources as faint as NGC 4388, the combination of ISGRI and JEM-X data might show in more detail the connection between the hard and soft X-rays, as seen in this work from simultaneous *INTEGRAL* and *RXTE* data. Another 500 ksec observation of 3C273 in AO-2 might give further insights into the cut-off of the NGC 4388 spectrum at high energies, e.g. when combined with the already existing data.

ACKNOWLEDGMENTS

This research has made use of the NASA/IPAC Extragalactic Database (NED) which is operated by the Jet Propulsion Laboratory.

REFERENCES

Antonelli, L. A., Matt, G., & Piro, L. 1997, A&A, 317, 686

Beckmann, V. 2002, proc. of the XXII Moriond Astrophysics Meeting "The Gamma-Ray Universe", eds. A. Goldwurm, D. Neumann, and J. Tran Thanh Van, p. 417

Boella, G., Butler, R. C., Perola, G.C., et al. 1997, A&AS, 122, 299

Butler, C., & Scarsi, L., 1990, SPIE, 1344, 46

Courvoisier, T.J.-L., Beckmann, V., Bourban, G., et al. 2003a, A&A, 411, L343

Courvoisier, T.J.-L., Walter, R., Beckmann, V., et al. 2003b, A&A, 411, L53

Diehl, R., Baby, N., Beckmann, V., et al. 2003, A&A, 411, L117

Fabian, A. C. 1977, Nature, 269, 672

Forster, K., Leighly, K. M., & Kay, L. E. 1999, ApJ, 523, 521

Frontera, F., Costa, E., & Dal Fiume, D. 1997, A&AS, 122, 357

Gehrels, N., Chipman, E., & Kniffen, D. A. 1993, A&AS, 97, 5

George, I. M., & Fabian, A. C. 1991, MNRAS, 249, 352

Ghisellini, G., Haardt, F., & Matt, G. 1994, MNRAS, 267, 743

Haardt, F., Maraschi, L., & Ghisellini, G. 1994, ApJ, 432, L95

Hanson, C. G., Skinner, G. K., Eyles, C. J., & Willmore, A. P. 1990, MNRAS, 242, 262

Iwasawa, K., Fabian, A. C., Ueno, S., et al. 1997, MNRAS, 285, 683

Iwasawa, K., Wilson, A. S., Fabian, A. C., Young, A. J. 2003, MNRAS, 345, 369

Jansen, F., Lumb, D., Altieri, B., et al. 2001, A&A, 365, L1

Johnson, W. N., Kinzer, R. L., Kurfess, J. D., et al. 1993, ApJS, 86, 693

Johnson, W.N., et al. 1994, in The 2nd Compton Observatory Symposium, C.E. Fichtel et al. (eds.) New York: AIP, p. 515

Lebrun, F., Ballet, J., Paul, J., et al. 1992, A&A 264, L22

Magdziarz, P., & Zdziarski, A. A. 1995, MNRAS, 273, 837

Malzac, J., & Petrucci, P.-O. 2002, MNRAS, 336, 1209

Markowitz, A., Edelson, R., & Vaughan, S. 2003, ApJ, 598, 935

Matt, G., Piro, L., Antonelli, L. A., et al. 1994, A&A, 292, L13

Paul, J., Ballet, J., Cantin, M., et al. 1991, Adv.Sp.Res. 11, 289

Petrucci, P. O., Haardt, F., Maraschi, L., et al. 2001, ApJ, 556, 716

Phillips, M. M., & Malin, D. F. 1982, MNRAS, 199, 905

Raymond, J. C., & Smith, B. W. 1977, ApJS, 35, 419

Risaliti, G. 2002, A&A, 386, 379

Sazonov, S., & Revnivtsev, M. 2004, A&A in press, astro-ph/0402415

Skinner, G., & Connell, P. 2003, A&A, 411, L123

Strüder, L., Briel, U., Dennerl, K., et al. 2001, A&A, 365, L18

Turner, M.J.L., Abbey, A., Arnaud, M., et al. 2001, A&A, 365, L27

Winkler, C., Courvoisier, T. J.-L., Di Cocco, G., et al. 2003, A&A, 411, L1